Article

Not peer-reviewed version

Mice Overexpressing Wild Type RRAS2: A Novel Preclinical Model for Testing Anti-Chronic Lymphocytic Leukemia Therapies

Balbino Alarcón *, Alejandro M. Hortal, Ana Villanueva, Irene Arellano, Cristina Prieto, Pilar Mendoza, Xose R Bustelo

Posted Date: 21 September 2023

doi: 10.20944/preprints202309.1417.v1

Keywords: R-RAS2; RAS; GTPases; chronic lymphocytic leukemia; B-CLL; mouse model; ibrutinib; venetoclax; new therapies; cancer treatment

Article

Mice Overexpressing Wild Type RRAS2: A Novel Preclinical Model for Testing Anti-Chronic Lymphocytic Leukemia Therapies

Alejandro M. Hortal [1,*], Ana Villanueva [1], Irene Arellano [1], Cristina Prieto [1], Pilar Mendoza [1], Xosé R. Bustelo [2] and Balbino Alarcón [1,*]

[1] Immune System Development and Function Program, Centro Biología Molecular Severo Ochoa, Consejo Superior de Investigaciones Científicas (CSIC)-Universidad Autónoma de Madrid, 28049 Madrid, Spain.
[2] Centro de Investigación del Cáncer, Instituto de Biología Molecular y Celular del Cáncer, and Centro de Investigación Biomédica en Red de Cáncer, CSIC and Universidad de Salamanca, 37007 Salamanca, Spain
* Correspondence: balarcon@cbm.csic.es, ahortal@cbm.csic.es

Abstract: B-cell chronic lymphocytic leukemia (B-CLL) is the most common type of leukemia in the Western world. Mutations in different genes, such as *TP53* and *ATM,* and deletions in specific chromosomal regions, including 11q or 17p, have been associated with a worse prognosis for the disease. Recent research from our group has demonstrated that, contrary to the usual cancer development process through missense mutations, B-CLL is driven by the overexpression of the small GTPase *RRAS2* in its wild-type form, without activating mutations. While some mouse models of this disease have been developed to date and are commonly used in B-CLL research, they come with various disadvantages, such as a long waiting period until the leukemia fully develops, the need for cell engraftment, or, in some cases, a failure to replicate the alterations found in human patients. We have recently introduced Rosa26-*RRAS2*$^{fl/fl}$xmb1-Cre as a new mouse model of B-CLL with full disease penetrance. In this work, we have validated this mouse model as a novel tool for the development of new therapies for B-CLL by testing two of the most widely applied targeted agents: ibrutinib and venetoclax. This also paves the way for the development of new targeted agents against R-RAS2 itself, an approach that has not yet been explored in clinical practice.

Keywords: R-RAS2; RAS; GTPases; chronic lymphocytic leukemia; B-CLL; mouse model; ibrutinib; venetoclax; new therapies; cancer treatment

1. Introduction

B-cell chronic lymphocytic leukemia (B-CLL) stands as the most common form of leukemia in the Western world [1], with an annual incidence rate of 3.1 and 6.1 per 100,000 in females and males, respectively [2]. Remarkable advancements in treatment and diagnosis have elevated the 5-year survival rate from 77.3% in 2009 to 87.9% today [3,4]. The median age at which B-CLL is diagnosed is 72 years [5,6]. Characterized by the accumulation of CD5+ B lymphocytes in the blood, spleen, and lymph nodes [7]. B-CLL exhibits CD5 expression in leukemic B cells, a marker typically found in T cells but uniquely present in B-CLL cells, distinguishing them from normal B cells [8]. Several genes, including *TP53*, *ATM*, *MYD88*, and those involved in Notch signaling, inflammatory pathways, B cell receptor signaling, and others, have been implicated in B-CLL development [9]. Additionally, genes regulating MAPK-ERK and MYC pathways have been connected to the disease [10]. Recurrent deletions in chromosomes 8p, 11q, 13q, and 17p, as well as trisomy of chromosome 12, have also been reported [9]. A 2022 study identified 82 additional putative driver mutations, each occurring in less than 2% of analyzed patients [11]. Notably, the currently known mutated genes mainly affect fewer than 10% of B-CLL patients, suggesting other alterations contribute to the disease. Prognostic biomarkers have become essential for assessing disease prognosis, encompassing host factors such as gender and age, cell marker expression levels (CD38, ZAP70, and CD49d), serological values (β2-

 doi:10.20944/preprints202309.1417.v1

microglobulin, LDH), genetic alterations (deletion of chromosome arms 11q, 13q, 17p, TP53 gene mutation, and trisomy 12), and the mutational status of the IGHV gene [12–14].

Traditionally, first-line therapy has relied on chemoimmunotherapy, such as FCR (fludarabine, cyclophosphamide, and rituximab), chlorambucil, or bendamustine with anti-CD20 antibodies (rituximab, obinutuzumab). However, long-term disease control with FCR is primarily achieved in patients with mutated IGHV genes. Recent years have witnessed a shift in treatment options, thanks to the development of kinase inhibitors targeting BCR signaling, such as ibrutinib (Bruton's tyrosine kinase (BTK)) and idelalisib (phosphoinositide 3-kinase (PI3K)δ) [15]. Second-generation, more specific BTK inhibitors (acalabrutinib), venetoclax (a specific inhibitor of the anti-apoptotic factor BCL2), alone or in combination with anti-CD20 antibodies, have further improved patient outcomes compared to traditional chemotherapy [16]. For instance, venetoclax treatment induces cell death independently of *TP53* mutations and/or del(17p) [17]. Ibrutinib has been highly successful in B-CLL treatment and is now a leading therapy, either alone or in combination with other chemotherapeutic or immunotherapeutic agents [18].

The widely used mouse model for B-CLL is the Eμ-TCL1 model, where the T-cell leukemia oncogene TCL1 is inserted under the control of the immunoglobulin heavy chain variable region promoter and immunoglobulin heavy chain enhancer (Eμ), resulting in B-CLL-like disease development at a late age (13 to 18 months) [19]. However, this model has drawbacks, including the extended period required for full disease development and its inability to fully represent the recurrent human B-CLL disease. Another approach involves engrafting the B-CLL cell line MEC-1 into Rag2-/-γc-/- mice, which mimics aggressive human B-CLL but falls short in expressing CD5, a canonical marker seen in human B-CLL patients [20]. Engraftment of B-CLL patient-derived B cells into NSG mice, with or without co-injection of polyclonally-activated autologous T cells pre-stimulated in vitro, has been successful but limits the window for B-CLL biology and potential treatment testing to just 63 days [21]. Deletion of the DLEU2/miR-15a/16-1 locus in mice, encoded on chromosome arm 13q, leads to an indolent disease mirroring human B-CLL characteristics, albeit with a disease penetrance of approximately 50% [22]. These and other approaches to the generation of mouse models of B-CLL are thoroughly reviewed in [23]. While these models are currently used in B-CLL research, there's a growing need for newer models that better capture the full heterogeneity of B-CLL biology. Hence, it is crucial in mouse model development to prioritize full B-CLL penetrance, eliminating the need for xenografts, and promoting disease development in the early stages of mouse life, thus avoiding prolonged waiting times for disease study.

The RAS protein family includes numerous small guanosine triphosphate hydrolases (GTPases), some of which have been found to be mutated and implicated in various human cancers [24]. The classical RAS members, K-RAS, H-RAS, and N-RAS, were discovered in the late 1960s, 1970s, and early 1980s [25]. RAS-related proteins (R-RAS) share several domains and regulatory factors with classical RAS proteins, mediating their activation and inactivation cycles, including guanine exchange factors (GEF) and GTPase activating proteins (GAP) [26]. Mutation of R-RAS2 in analogous residues to G12V and Q61L in classical RAS proteins has induced comparable cell transformation in culture and tumor growth in mice [27,28]. A key distinction is the high intrinsic nucleotide exchange activity of R-RAS2, allowing it to exchange GDP for GTP independently of specific GEF proteins at rates similar to those observed with H-RAS after GEF addition [29].

R-RAS2 plays diverse roles in the body. It regulates platelet activation by interacting with the glycoprotein VI-ITAM-containing collagen receptor [30]. R-RAS2 regulates Schwann cell migration [31]. and mammary gland development [32]. Overexpression of R-RAS2 protein has been observed in various cancer types, including oral squamous cell carcinoma [33], esophageal tumors [34], hepatocellular carcinoma, [35] and highly aggressive skin cancer [36]. Mutation or overexpression of *RRAS2* has led to the transformation of breast cell lines [37] [38]. R-RAS2 with the Q72L mutation, associated with Noonan Syndrome, has been found to trigger the formation of various tumors [39,40]. Recent reports have shown that R-RAS2 harboring the Q72L mutation is a potent oncogenic driver that triggers the formation of a wide variety of tumors (ovarian cystadenomas, T-ALL, etc.) [41].

Preprints (www.preprints.org) | NOT PEER-REVIEWED | Posted: 21 September 2023 doi:10.20944/preprints202309.1417.v1

Moreover, other mutations (G23V/A/C/S, G24D/C/V, A70T, and Q72H) in human cancer have shown transforming potential when expressed in immortal cell lines [42].

Previous research from our group has demonstrated that R-RAS2 directly interacts with both B-cell and T-cell receptors (BCR and TCR) through their immunoreceptor tyrosine-based activation motif (ITAM), predominantly in the inactive GDP-bound state of R-RAS2. This interaction provides tonic survival signals [43]. R-RAS2 also regulates the internalization of the TCR following immune synapse formation, but only in its wild-type (WT) form [44]. In B cells, R-RAS2 plays a crucial role in governing the proper formation of germinal centers by influencing B-cell metabolism [45]. Through the analysis of human samples from B-CLL patients and utilizing our Rosa26-*RRAS2*$^{fl/fl}$-mb1-Cre (and Sox2-Cre) mouse models, we have recently demonstrated that the overexpression of RRAS2 drives the development of B-CLL [46]. In our current study, we treated Rosa26-*RRAS2*$^{fl/fl}$-mb1-Cre with the clinically used drugs, ibrutinib and venetoclax [16]. Notably, the leukemic cell population, especially in the case of ibrutinib treatment, showed significant regression. This suggests the potential utility of this mouse model as a valuable tool for exploring new therapeutic approaches for B-CLL.

2. Materials and Methods

2.1. Mice

The Rosa26-*RRAS2*$^{fl/fl}$ knock-in mouse line was established on a C57Bl/6J genetic background. It was generated with genOway technologies, by the homologous recombination of a cassette containing the coding sequence for human R-RAS2 tagged with HA in the Rosa26 locus. This construct is based on the CTV vector (a gift from Klaus Rajewsky; Addgene plasmid #15912; http://n2t.net/addgene:15912; RRID:Addgene_15,912) [47] and its detailed composition is explained in [46]. This mouse line was crossed with mb1-Cre mice. These mice express the Cre recombinase specifically in B cells starting at an early precursor phase, since the *mb1* gene encodes the Igα signaling subunit of the BCR. Thereby, we achieve B-cell specific overexpression of *RRAS2*. Previously described mb1-Cre transgenic mouse lines were gently provided by Prof. Dr. Michael Reth (University of Freiburg, Germany) [48]. All mice were maintained under SPF conditions at the animal facility of the Centro de Biología Molecular Severo Ochoa (CBMSO) in accordance with national and European guidelines. All the procedures were approved by the ethical committee of the CBMSO and were under the Community of Madrid authorization numbers PROEX 384/15 and PROEX 296.7/21.

2.2. Cell preparation

Spleen from mice were homogenized with 40 µm strainers (Falcon) and washed in phosphate-buffered saline (PBS) containing 2% FBS. Bone marrows were extracted from the tibias of mice by removing the proximal tibia and centrifuging at maximum speed for 30s. Blood was extracted from the facial vein by puncture and the blood was kept anticoagulated in an excess of 30µl of heparin (1000UI/ml) (Chiesi). Spleen, bone marrow and blood cells were resuspended for 5 min in ACK buffer (0.15 M NH_4Cl, 10 mM $KHCO_3$, 0.1 mM EDTA, pH 7.2–7.4) to lyse and discard the erythrocytes and washed in PBS with 2% FBS. Cells were subsequently analyzed by flow cytometry after staining with the appropriate fluorescently labelled antibodies.

2.3. Mouse drug treatment

Twenty-three to twenty-seven week-old Rosa26-*RRAS2*$^{fl/fl}$xmb1-Cre mice were treated with either vehicle, ibrutinib at 25 mg/Kg or venetoclax at 50 mg/Kg for 31 days. Drugs were dissolved in a solution of 4% DMSO (Sigma-Aldrich), 80% Kollisolv® PEG E 400 (Sigma-Aldrich), 4% Tween 20 (Sigma-Aldrich) and 12% saline solution. 200µl were administered by oral gavage every day to each mouse of 25g of weight, adjusting the volume for heavier or lighter mice. Mice were bled at the start, the end and halfway through the experiment from the facial vein and cells were stained and analyzed by flow cytometry to track the evolution of the tumoral cells. At the experiment endpoint, all mice were sacrificed by CO_2 inhalation and spleen and bone marrow were extracted. Bone marrow and

 doi:10.20944/preprints202309.1417.v1

blood were used in their entirety for flow cytometry analysis and the spleens were cut in half so that one part could be used for cytometry analysis and the other half, for hematoxylin/eosin staining.

2.4. Flow cytometry

Mouse and human single-cell suspensions were incubated with Ghost dye 540 (TONBO Biosciences) at 1:500 dilution for 15min in PBS to label and discard dead cells. After that, cells were incubated with fluorescently labelled antibodies for 30 min at 4 °C after blocking FC receptors using anti-CD16/32 antibody (1:250) for 15 min at 4 °C. Both of these steps are carried out in PBS + 2% FBS. The utilized fluorophore-labelled antibodies were anti-CD5-PE, anti-CD19-PECy7, anti-IgM-APC, anti-B220-APCCy7 and anti-IgD-eF450, all from BD Pharmingen. Afterwards, cells were washed in PBS + 2% FBS and data were collected on a FACS Canto II (Becton Dickinson) cytometer. A minimum of 50,000 and a maximum of 200,000 events was acquired in every measurement. Analyses were performed using FlowJo software (TreeStar). Counting of total cells was performed with CountBright™ beads (Invitrogen).

2.5. Hematoxylin and eosin staining

Spleens from Rosa26-*RRAS2*$^{fl/fl}$xmb1-Cre mice were fixed in formalin solution, neutral buffered, 10% (Sigma) overnight at 4ºC immediately after sacrificing the mice. They were then washed with PBS and sent to the Histology service at the Centro Nacional de Biotecnología (Madrid, Spain), where the hematoxylin/eosin staining was carried out. Images of the stainings were captured using a vertical AxioImager M1 microscope (Zeiss). Follicle areas were calculated using the formula π*a*b, being a and b the two radii of the ellipse. All follicles visible in their entirety were used to calculate the areas in three representative images per mouse.

2.5. Statistical analysis

Statistical parameters including the exact value of n, the mean +/− S.E.M. are described in the Figures and Figure legends. Two-tailed unpaired t test with Welch's correction and two-way ANOVA tests were used as indicated to assess the significance of mean differences. The number of mice to be used for comparison was calculated from preliminary experiments aimed to generate significant data using a two-sided t-test with alpha = 0.05 and a standard deviation of about 0.3. Outliers for the different analyses were identified using ROUT model at Q=1% to remove definite outliers from analysis. All data was analyzed using the GraphPad Prism 10 software.

3. Results

3.1. Testing the Rosa26-RRAS2$^{fl/fl}$xmb1-Cre Mouse Model of CLL in Response to Ibrutinib and Venetoclax

To validate the Rosa26-*RRAS2*$^{fl/fl}$xmb1-Cre mouse model for preclinical testing of new compounds in the context of B-cell chronic lymphocytic leukemia (B-CLL), we conducted experiments with two commonly used molecular targeted therapies: ibrutinib [15,16] and venetoclax [16,17]. We divided 23 to 27-week-old Rosa26-*RRAS2*$^{fl/fl}$xmb1-Cre mice with comparable levels of circulating leukemic CD19+CD5+ cells into three groups, each comprising 9 mice. These mice received daily single doses of ibrutinib, venetoclax, or a vehicle control via oral gavage, as outlined in Figure 1a. At an intermediate time point (18 days of treatment), we collected blood samples to assess the drugs' impact on circulating leukemic cells. All mice were euthanized on day 31 to evaluate the effects of drug treatment on leukemic cells in the blood, spleen, and bone marrow. Unfortunately, both drug administration regimens led to toxicity in some animals, resulting in the mortality of 3 out of 9 mice in the ibrutinib group and 4 out of 9 mice in the venetoclax group by day 18. No further drug-related deaths occurred up to day 31 (Figure 1b). Despite this, there were no significant changes in body weight among the remaining treated mice (Figure 1c). However, a general assessment of the mice's condition revealed that those undergoing ibrutinib and, to a greater extent, venetoclax

Preprints (www.preprints.org) | NOT PEER-REVIEWED | Posted: 21 September 2023 doi:10.20944/preprints202309.1417.v1

treatment exhibited mild lethargy as treatment progressed, compared to those receiving the vehicle alone.

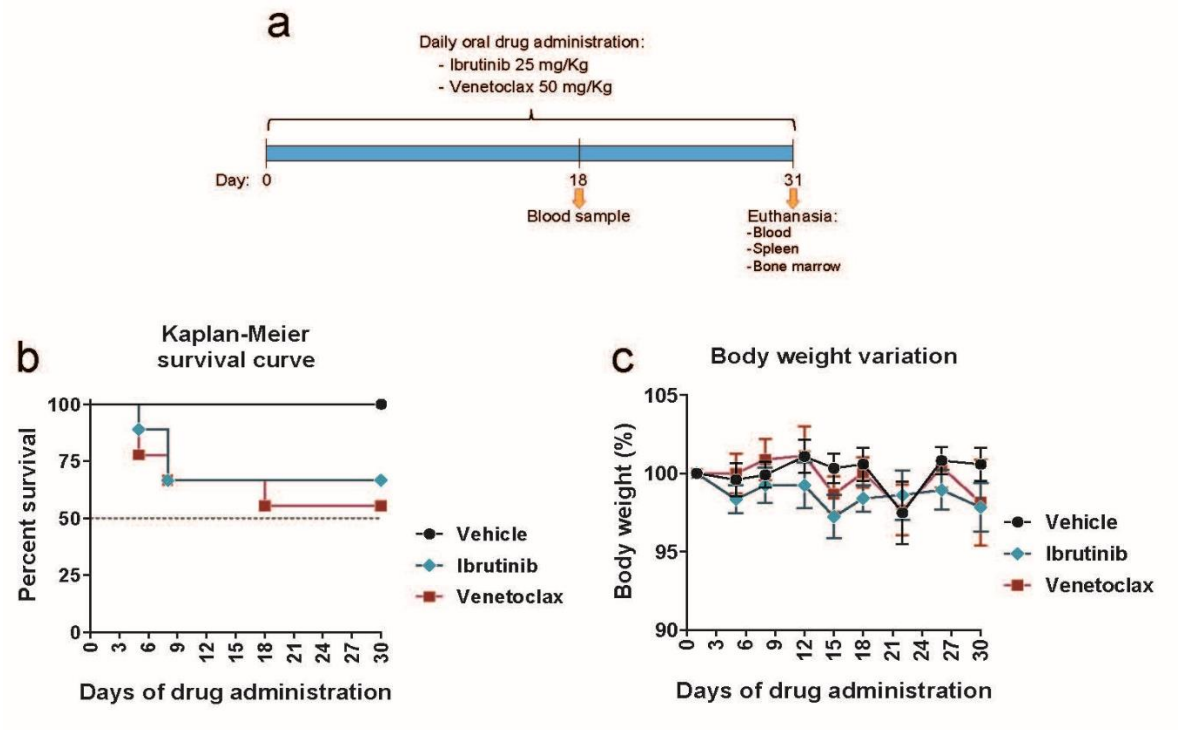

Figure 1. Rosa26-*RRAS2*$^{fl/fl}$xmb1-Cre mice can go through a one-month long treatment with ibrutinib or venetoclax. a) Schematic representation of the treatment protocol used in Rosa26-*RRAS2*$^{fl/fl}$xmb1-Cre mice. **b)** Kaplan-Meier survival curve of the mice under treatment. n=9 mice per group started the experiment. **c)** Relative percentage of mouse weight evolution through the course of the treatment.

Following euthanasia on day 31, we assessed the effects of drug treatment on lymphoid organs. Both drug treatments significantly reduced spleen weight (Figure 2a), which is noteworthy given our previous findings of *RRAS2* overexpression leading to splenomegaly [46]. Venetoclax treatment resulted in a significant decrease in the number of total CD19+ B cells, whereas ibrutinib treatment did not affect the number of total B cells in the spleen (Figure 2b). We then examined the effects on leukemic B cells characterized by the CD5 marker. Neither treatment significantly reduced the percentage or number of CD19+CD5+ leukemic B cells (Figure 2c), although ibrutinib showed a partial reduction in this population. The construct used for inserting the human *RRAS2* gene into the Rosa26 locus of mice includes an IRES sequence, allowing for the co-transcription of the green marker GFP along with R-RAS2 [46]. Consequently, GFP expression serves as a marker of *RRAS2* overexpression in B cells. Only venetoclax treatment led to a reduction in the percentage and number of GFP+ CD19+ B cells, with statistical significance observed only for cell numbers. In contrast, ibrutinib treatment had no effect on the abundance of GFP+ CD19+ cells (Figure 2d).

Preprints (www.preprints.org) | NOT PEER-REVIEWED | Posted: 21 September 2023 doi:10.20944/preprints202309.1417.v1

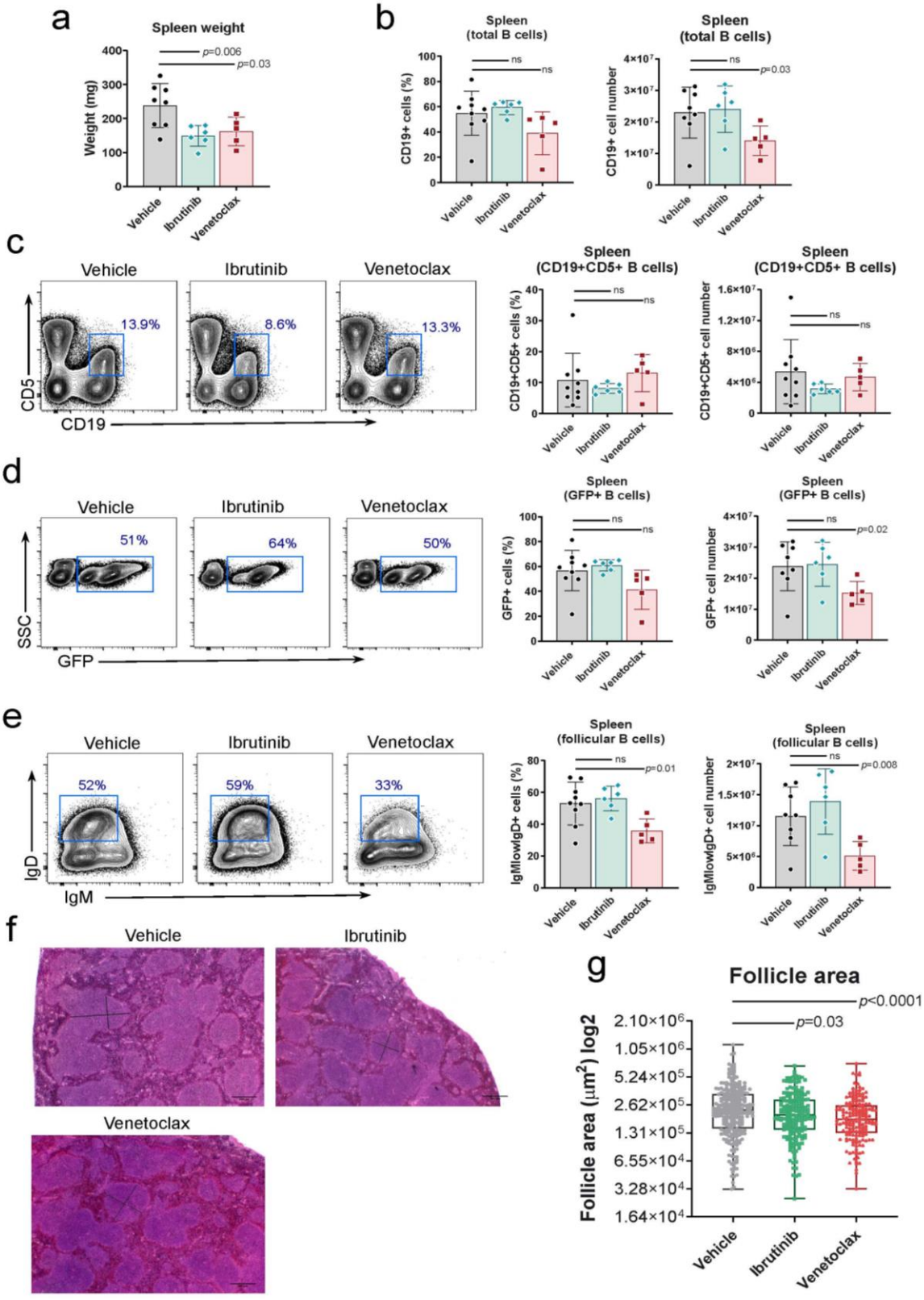

Figure 2. Ibrutinib and venetoclax treatment reverse the splenomegaly and follicle enlargement induced by *RRAS2* overexpression. a) Spleen weights of mice in the vehicle, ibrutinib and venetoclax treatment groups at the experiment endpoint, day 31. Two-tailed unpaired t test with Welch's correction. b) Quantification of the number of CD19+ B cells in the spleens of the treated mice at the experiment endpoint. Two-tailed unpaired t test with Welch's correction. Left, percentage of the total lymphocyte population; right, total numbers. c) Left, representative two-parameter flow cytometry

 doi:10.20944/preprints202309.1417.v1

plots of CD19 and CD5 expression in the spleens of mice in each of the three established groups. The CD19+CD5+ population is highlighted with a blue box. Right, quantification of the number of CD19+CD5+ B cells in the spleens of the treated mice at the experiment endpoint. Left graph, percentage of the total lymphocyte population; right graph, total numbers. Two-tailed unpaired t test with Welch's correction. d) Left, representative two-parameter flow cytometry plots of GFP expression vs side scatter (SSC) in the spleens of mice in each of the three established groups. The GFP+ population is highlighted with a blue box. Right, quantification of the number of GFP+ cells in the spleens of the treated mice at the experiment endpoint. Left graph, percentage of the total lymphocyte population; right graph, total numbers. Two-tailed unpaired t test with Welch's correction. e) Left, representative two-parameter flow cytometry plots of IgM and IgD expression within the total CD19+ B cell population. The follicular IgMlowIgD+ population is highlighted with a blue box. Right, quantification of the number of IgMlowIgD+ cells with the CD19+ gate in the spleens of the treated mice at the experiment endpoint. Left graph, percentage of the total CD19+ population; right graph, total numbers. Two-tailed unpaired t test with Welch's correction. f) Representative hematoxylin and eosin stainings of the spleens of mice in the vehicle, ibrutinib and venetoclax groups at the experiment endpoint. Scale bars represent 400μm. In each of the three images, the black bars are illustrative of the diameters used to calculate follicle areas. g) Box and whiskers plot showing all points and median value of the quantification of follicle areas using the diameters illustrated in the images in f). Areas were calculated for all follicles visible in their entirety in three representative images per mouse. n=9 in the vehicle group, n=6 in the ibrutinib group, n=5 in the venetoclax group. Two-tailed unpaired t test with Welch's correction. ns: not significant.

Leukemic B-CLL B cells typically express both membrane IgM and IgD as their B cell antigen receptors [49], with higher IgM expression, especially in patients with unmutated IGHV genes, which indicates a worse disease prognosis [49]. Venetoclax, but not ibrutinib, treatment significantly reduced the number of follicular B cells in Rosa26-*RRAS2*$^{fl/fl}$xmb1-Cre mice (Figure 2e), suggesting venetoclax's potential toxicity toward healthy B cell populations. Given that both ibrutinib and venetoclax reduced splenomegaly (Figure 2a), we examined their effects on the size of spleen follicles, which are the sites for normal and malignant B cell localization and maturation. As previously described [46], we found that control Rosa26-*RRAS2*$^{fl/fl}$xmb1-Cre mice treated with the vehicle alone exhibited abnormally large follicles (Figure 2f). Quantitative analysis of the area occupied by each follicle in different spleen sections revealed that both ibrutinib and venetoclax treatments significantly reduced follicle size, with venetoclax showing a more pronounced effect (Figure 2g). In summary, both ibrutinib and venetoclax reduced splenomegaly and the size of spleen follicles but did not significantly impact the frequency and size of the leukemic CD19+CD5+ population in the spleen. However, venetoclax appeared to have a toxic effect on non-leukemic follicular B cells.

We also assessed the bone marrow for the presence of leukemic cells and the effects of drug treatments. Ibrutinib did not significantly reduce the number of GFP+ CD19+ B cells (Figure 3a) or CD19+CD5+ B cells in the bone marrow (Figure 3b), suggesting that this drug did not influence bone marrow infiltration by leukemic cells. For venetoclax, a small reduction in the number of both GFP+ CD19+ B cells (Figure 3a) and CD19+ CD5+ B cells (Figure 3b) was observed, though without statistical significance. The impact of both drug treatments on B cell precursor generation in the bone marrow, based on B220 and IgM marker expression, indicated that venetoclax treatment led to a significant reduction in the number of immature B220^{high}IgM+ B cells but not in the number of B220^{int}IgM^{-} pro-pre-B cells (Figure 3c), suggesting a partial blockade in normal pro-pre-B cell to immature B cell differentiation. In contrast, ibrutinib treatment did not affect B-cell maturation in the bone marrow (Figure 3c). The B-cell maturation blockade induced by venetoclax may explain the observed partial reduction in GFP+ CD19+ and CD19+ CD5+ cells in the bone marrow (Figure 3a and 3b, respectively) and the decrease in total CD19+ and GFP+ B cells in the spleen (Figure 2b and 2d, respectively).

Preprints (www.preprints.org) | NOT PEER-REVIEWED | Posted: 21 September 2023 doi:10.20944/preprints202309.1417.v1

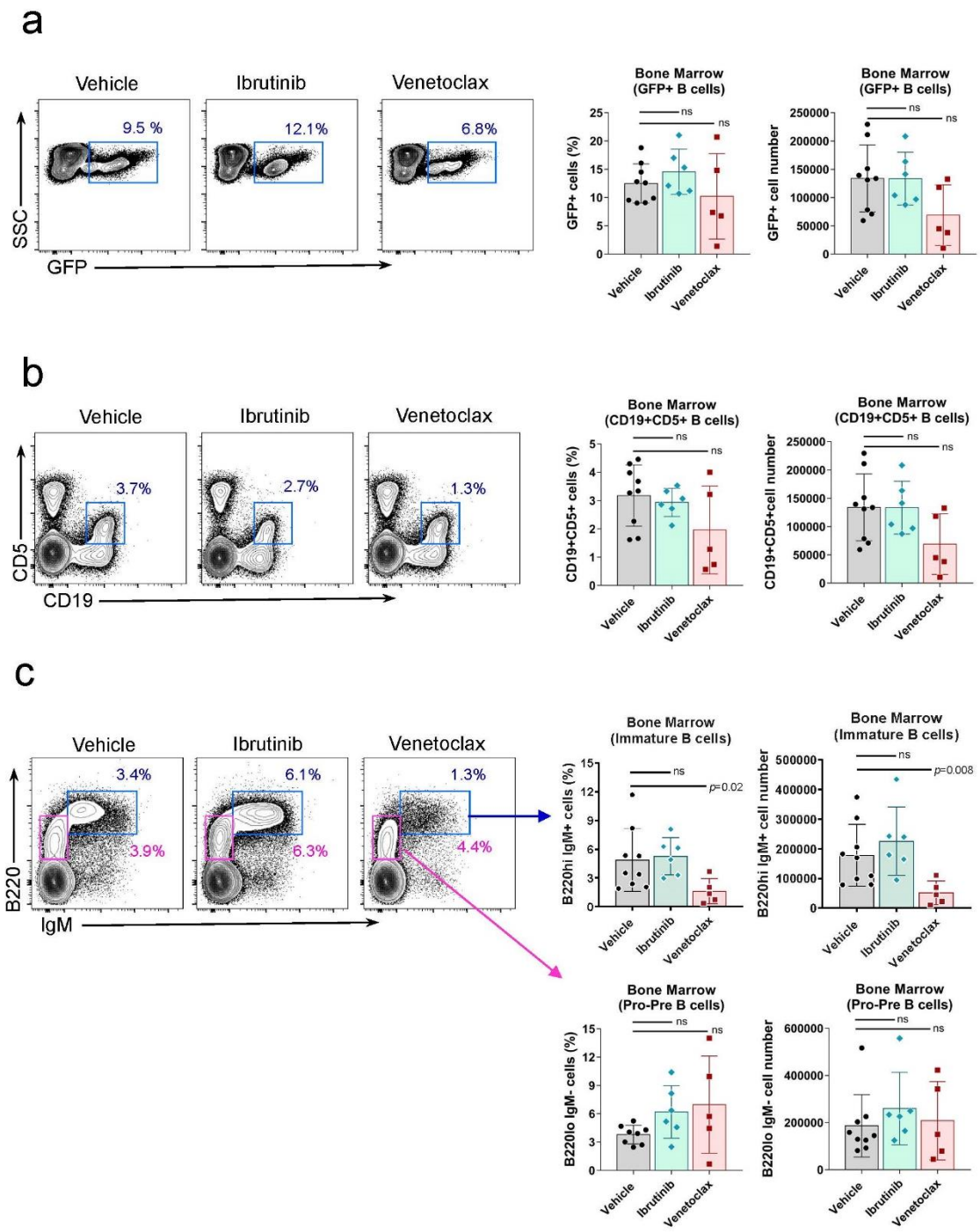

Figure 3. Venetoclax treatment hampers transition from pro-pre B to immature cell stage in the bone marrow. a) Left, representative two-parameter flow cytometry plots of GFP expression vs side scatter (SSC) in the bone marrow of mice in each of the three established groups. The GFP+ population is highlighted with a blue box. Right, quantification of the number of GFP+ cells in the bone marrow of the treated mice at the experiment endpoint. Left graph, percentage of the total lymphocyte population; right graph, total numbers. Two-tailed unpaired t test with Welch's correction. **b)** Left, representative two-parameter flow cytometry plots of CD19 and CD5 expression in the bone marrow of mice in each of the three established groups. The CD19+CD5+ population is highlighted with a blue box. Right, quantification of the number of CD19+CD5+ cells in the bone marrow of the treated mice at the experiment endpoint. Left graph, percentage of the total lymphocyte population; right graph, total numbers. Two-tailed unpaired t test with Welch's correction. **c)** Left, representative two-parameter flow cytometry plots of IgM and B220 expression within the total CD5- population in the bone marrow of mice in each of the three established groups. The immature B220hi IgM+ population

 doi:10.20944/preprints202309.1417.v1

is highlighted with a blue box. The pro-pre B cell population is highlighted with a pink box. Right, top graphs, quantification of the number of immature B cells in the bone marrow of the treated mice at the experiment endpoint. Left graph, percentage of the total CD5- population; right graph, total numbers. Right, bottom graphs, quantification of the number of pro-pre B cells in the bone marrow of the treated mice at the experiment endpoint. Left graph, percentage of the total CD5- population; right graph, total numbers. Two-tailed unpaired t test with Welch's correction. ns: not significant.

We further analyzed the progressive efficacy of ibrutinib and venetoclax treatments in peripheral blood at day 18 and the experiment endpoint at day 31. While venetoclax treatment showed a trend toward reducing the total number of B cells at both time points, this difference was not statistically significant (Figure 4a). This phenotype likely reflects the observed pro-pre-B to immature B cell maturation blockade in the bone marrow after venetoclax treatment (Figure 3c). Analysis of the number of leukemic B cells based on CD5 marker expression by CD19+ B cells (Figure 4b) did not reveal significant effects in the overall analysis (Figure 4c). However, when focused on the total CD19+ B cell gate (Figure 4d), significant differences were observed in the behavior of leukemic $B220^{low}$CD5+ and normal, healthy B220+CD5- B cells. Leukemic $B220^{low}$CD5+ cells showed opposite dynamics between ibrutinib-treated mice and venetoclax-treated or control groups. By day 18, the percentage of leukemic cells in ibrutinib-treated mice decreased compared to the experiment's start, whereas both venetoclax-treated and vehicle-only mice exhibited an increase in this population. This effect was more pronounced by day 31 (Figure 4e). In this analysis, the significant difference between ibrutinib and venetoclax-treated mice is primarily due to initial heterogeneity at the start of the procedure (Figure 4e). When considering the starting point as 100% for all three cases and measuring the relative evolution of $B220^{low}$CD5+ cells, the distinct dynamics between ibrutinib and venetoclax and the control group become more evident (Figure 4f). Confirming the specific effect of ibrutinib on circulating B cells, we observed an opposite effect in the normal B220+CD5- B cell population. Ibrutinib resulted in a progressive increase in the percentage of this population, whereas mice administered venetoclax or the vehicle showed a reduction in these cells (Figure 4g). These results, in conjunction with findings in the spleen (Figure 2e), indicated that ibrutinib treatment caused a significant increase in the normal follicular IgM^{low} IgD+ B cell population in the blood, while venetoclax had no impact on this characteristic (Figure 4h).

Preprints (www.preprints.org) | NOT PEER-REVIEWED | Posted: 21 September 2023 doi:10.20944/preprints202309.1417.v1

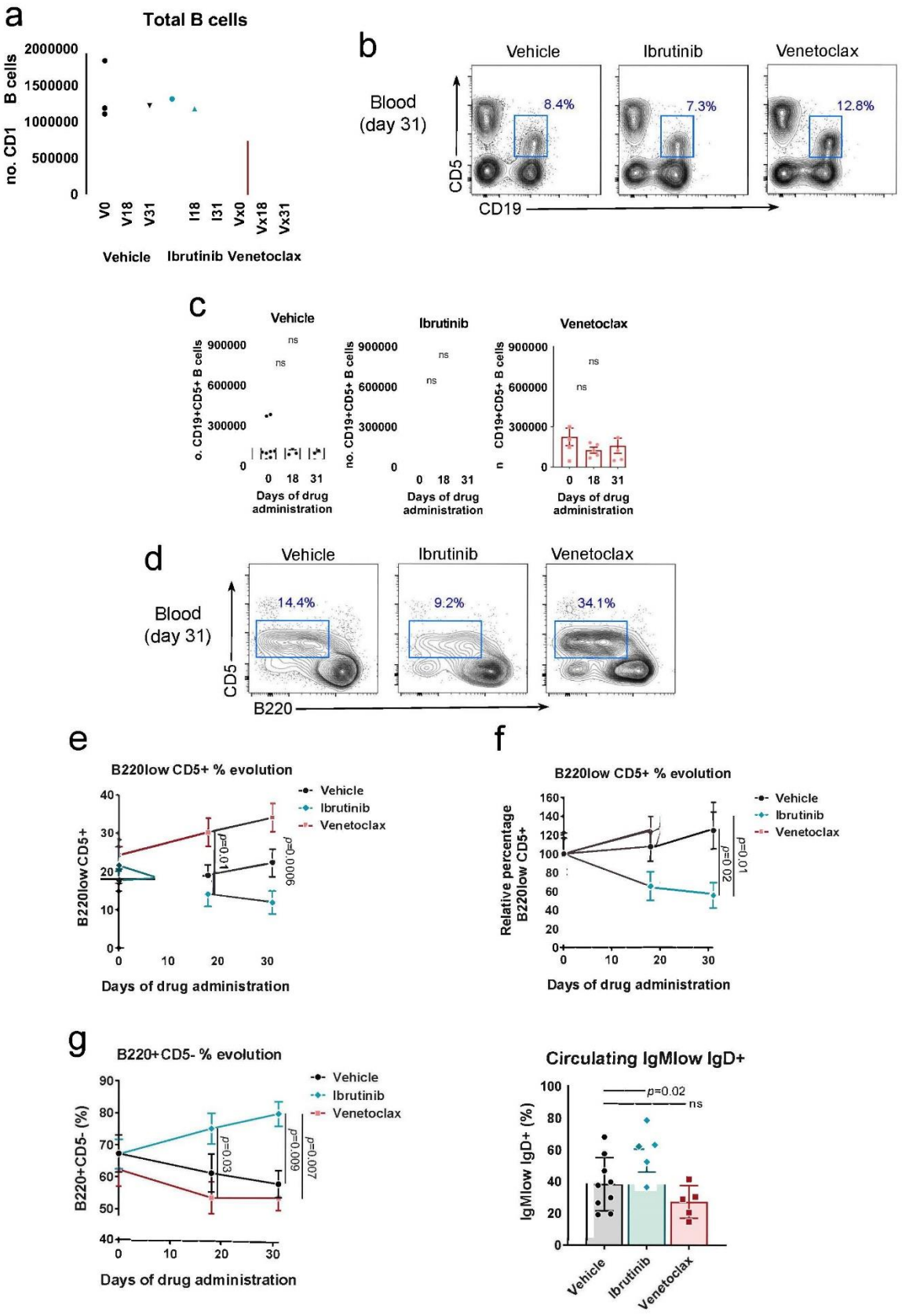

Figure 4. Ibrutinib treatment reduces the circulating CD19+B220lowCD5+ leukemic population in the blood of Rosa26-*RRAS2*$^{fl/fl}$xmb1-Cre mice. a) Quantification of the total number of CD19+ B cells in the blood of mice at the start (0), halfway through the experiment (18) and the experiment endpoint (31) in the vehicle, ibrutinib and venetoclax groups. Column bars represent mean values ± SEM. b) Representative two-parameter flow cytometry plots of CD19 and CD5 expression in the blood of mice

 doi:10.20944/preprints202309.1417.v1

in each of the three established groups at the experiment endpoint. The CD19+CD5+ population is highlighted with a blue box. c) Quantification of the total number of CD19+CD5+ leukemic B cells in the blood of mice at the start (0), halfway through the experiment (18) and the experiment endpoint (31) in the vehicle, ibrutinib and venetoclax groups. d) Representative two-parameter flow cytometry plots of B220 and CD5 expression within the total CD19+ population at the endpoint of the experiment in the blood of the three established groups. The B220lowCD5+ population is highlighted with a blue box. e) B220lowCD5+ leukemic cells evolution, within the total CD19+ gate, in the blood of treated mice. Two-way ANOVA test. f) B220lowCD5+ population shown in e) relative evolution through the course of treatment. Two-way ANOVA test. g) B220+CD5- cells evolution, within the total CD19+ gate, in the blood of treated mice. Two-way ANOVA test. h) IgMlow IgD+ population, within the total CD19+ cells, in the blood of mice at the endpoint of the experiment. Two-tailed unpaired t test with Welch's correction. ns: not significant.

4. Discussion

There are limited mouse models that fully replicate B-CLL, with the Eμ-TCL1 being the most commonly used. However, this model presents challenges, such as a long disease development period (3 to 5 months for spleen involvement and over a year for blood disease) and the need for genetic engineering to insert the TCL1 oncogene [19]. Alternative methods include xenografts using the B-CLL cell line MEC-1 [20], co-transplantation of patient-derived B-CLL B cells with autologous pre-stimulated T cells [21], or deletion of the DLEU2/miR-15a/16-1 locus in mice to mimic indolent B-CLL [22].

In contrast, the Rosa26-*RRAS2*$^{fl/fl}$xmb1-Cre mouse model [46] offers a novel approach. It exhibits early onset of CD19+CD5+ leukemic cells with a 100% disease penetrance, concurrent with splenomegaly and progressive blood lymphocytosis leading to reduced lifespan [46]. In this study, we validate the Rosa26-*RRAS2*$^{fl/fl}$xmb1-Cre model for preclinical testing of B-CLL therapies. Treatment of these mice with venetoclax and, notably, ibrutinib leads to a reduction in CD19+B220^{low}CD5+ leukemic cells in the blood and spleen.

However, it's worth noting that the treatments caused the mortality of 3 out of 9 mice in the ibrutinib group and 4 out of 9 in the venetoclax group by day 18, reflecting side effects seen in some B-CLL patients [51]. In one case, a mouse treated with venetoclax had to be sacrificed due to severe lymphocyte loss. Venetoclax also significantly reduced the population of immature B cells in the bone marrow, which may explain the loss of B cells in some cases. Such side effects emphasize the need for therapies that balance efficacy with reduced side effects.

The splenomegaly observed in the Rosa26-RRAS2fl/flxmb1-Cre mice mirrors the human condition [5]. After one month of ibrutinib and venetoclax treatment, splenomegaly was significantly reduced, consistent with the effects seen in B-CLL patients [53,54]. These observations highlight the relevance of this mouse model for studying B-CLL and its response to treatment. In future studies, gender-related effects on treatment efficacy should be evaluated, as B-CLL affects male patients approximately twice as often as females [2].

An unexplored treatment option for B-CLL and other malignancies is the use of direct R-RAS2 inhibitors. As demonstrated previously [46], overexpression of WT *RRAS2* drives B-CLL development. Therefore, targeting R-RAS2 directly is a promising avenue for further research. Direct inhibitors, administered alone or in combination with other therapies like ibrutinib, may enhance therapeutic efficacy and reduce the risk of ibrutinib resistance [57,58].

5. Conclusions

In summary, we have validated the use of Rosa26-*RRAS2*$^{fl/fl}$xmb1-Cre mice as a novel model for preclinical B-CLL drug testing. This opens the door to developing new drugs targeting R-RAS2 and exploring combination therapies for improved treatment outcomes.

References

1. Bosch, F.; Dalla-Favera, R. Chronic Lymphocytic Leukaemia: From Genetics to Treatment. *Nat. Rev. Clin. Oncol.* **2019**, *16*, 684–701, doi:10.1038/s41571-019-0239-8.
2. Siegel, R.L.; Miller, K.D.; Jemal, A. Cancer Statistics, 2017. *CA. Cancer J. Clin.* **2017**, *67*, 7–30, doi:10.3322/caac.21387.
3. Bailey, C.; Richardson, L.C.; Allemani, C.; Bonaventure, A.; Harewood, R.; Moore, A.R.; Stewart, S.L.; Weir, H.K.; Coleman, M.P.; Members), C.W.G. (US Adult Leukemia Survival Trends in the United States by Subtype: A Population-Based Registry Study of 370,994 Patients Diagnosed during 1995-2009. *Cancer* **2018**, *124*, 3856–3867, doi:10.1002/cncr.31674.
4. Chronic Lymphocytic Leukemia - Cancer Stat Facts Available online: https://seer.cancer.gov/statfacts/html/clyl.html (accessed on 16 September 2022).
5. Eichhorst, B.; Robak, T.; Montserrat, E.; Ghia, P.; Niemann, C.U.; Kater, A.P.; Gregor, M.; Cymbalista, F.; Buske, C.; Hillmen, P.; et al. Chronic Lymphocytic Leukaemia: ESMO Clinical Practice Guidelines for Diagnosis, Treatment and Follow-Up. *Ann. Oncol.* **2021**, *32*, 23–33, doi:10.1016/j.annonc.2020.09.019.
6. Hallek, M.; Shanafelt, T.D.; Eichhorst, B. Chronic Lymphocytic Leukaemia. *The Lancet* **2018**, *391*, 1524–1537, doi:10.1016/S0140-6736(18)30422-7.
7. Ghia, P.; Ferreri, A.M.; Caligaris-Cappio, F. Chronic Lymphocytic Leukemia. *Crit. Rev. Oncol. Hematol.* **2007**, *64*, 234–246, doi:10.1016/j.critrevonc.2007.04.008.
8. Gary-Gouy, H.; Sainz-Perez, A.; Marteau, J.-B.; Marfaing-Koka, A.; Delic, J.; Merle-Beral, H.; Galanaud, P.; Dalloul, A. Natural Phosphorylation of CD5 in Chronic Lymphocytic Leukemia B Cells and Analysis of CD5-Regulated Genes in a B Cell Line Suggest a Role for CD5 in Malignant Phenotype1. *J. Immunol.* **2007**, *179*, 4335–4344, doi:10.4049/jimmunol.179.7.4335.
9. Landau, D.A.; Carter, S.L.; Stojanov, P.; McKenna, A.; Stevenson, K.; Lawrence, M.S.; Sougnez, C.; Stewart, C.; Sivachenko, A.; Wang, L.; et al. Evolution and Impact of Subclonal Mutations in Chronic Lymphocytic Leukemia. *Cell* **2013**, *152*, 714–726, doi:10.1016/j.cell.2013.01.019.
10. Landau, D.A.; Tausch, E.; Taylor-Weiner, A.N.; Stewart, C.; Reiter, J.G.; Bahlo, J.; Kluth, S.; Bozic, I.; Lawrence, M.; Böttcher, S.; et al. Mutations Driving CLL and Their Evolution in Progression and Relapse. *Nature* **2015**, *526*, 525–530, doi:10.1038/nature15395.
11. Knisbacher, B.A.; Lin, Z.; Hahn, C.K.; Nadeu, F.; Duran-Ferrer, M.; Stevenson, K.E.; Tausch, E.; Delgado, J.; Barbera-Mourelle, A.; Taylor-Weiner, A.; et al. Molecular Map of Chronic Lymphocytic Leukemia and Its Impact on Outcome. *Nat. Genet.* **2022**, 1–11, doi:10.1038/s41588-022-01140-w.
12. Hallek, M.; Wanders, L.; Ostwald, M.; Busch, R.; Senekowitsch, R.; Stern, S.; Schick, H.-D.; Kuhn-Hallek, I.; Emmerich, B. Serum B2-Microglobulin and Serum Thymidine Kinase Are Independent Predictors of Progression-Free Survival in Chronic Lymphocytic Leukemia and Immunocytoma. *Leuk. Lymphoma* **1996**, *22*, 439–447, doi:10.3109/10428199609054782.
13. Cohen, J.A.; Bomben, R.; Pozzo, F.; Tissino, E.; Härzschel, A.; Hartmann, T.N.; Zucchetto, A.; Gattei, V. An Updated Perspective on Current Prognostic and Predictive Biomarkers in Chronic Lymphocytic Leukemia in the Context of Chemoimmunotherapy and Novel Targeted Therapy. *Cancers* **2020**, *12*, 894, doi:10.3390/cancers12040894.
14. Rassenti, L.Z.; Jain, S.; Keating, M.J.; Wierda, W.G.; Grever, M.R.; Byrd, J.C.; Kay, N.E.; Brown, J.R.; Gribben, J.G.; Neuberg, D.S.; et al. Relative Value of ZAP-70, CD38, and Immunoglobulin Mutation Status in Predicting Aggressive Disease in Chronic Lymphocytic Leukemia. *Blood* **2008**, *112*, 1923–1930, doi:10.1182/blood-2007-05-092882.
15. Burger, J.A.; Chiorazzi, N. B Cell Receptor Signaling in Chronic Lymphocytic Leukemia. *Trends Immunol.* **2013**, *34*, 592–601, doi:10.1016/j.it.2013.07.002.
16. Awan, F.T.; Al-Sawaf, O.; Fischer, K.; Woyach, J.A. Current Perspectives on Therapy for Chronic Lymphocytic Leukemia. *Am. Soc. Clin. Oncol. Educ. Book* **2020**, 320–329, doi:10.1200/EDBK_279099.
17. Anderson, M.A.; Deng, J.; Seymour, J.F.; Tam, C.; Kim, S.Y.; Fein, J.; Yu, L.; Brown, J.R.; Westerman, D.; Si, E.G.; et al. The BCL2 Selective Inhibitor Venetoclax Induces Rapid Onset Apoptosis of CLL Cells in Patients via a TP53-Independent Mechanism. *Blood* **2016**, *127*, 3215–3224, doi:10.1182/blood-2016-01-688796.
18. Lucas, F.; Woyach, J.A. Inhibiting Bruton's Tyrosine Kinase in CLL and Other B-Cell Malignancies. *Target. Oncol.* **2019**, *14*, 125–138, doi:10.1007/s11523-019-00635-7.
19. Bichi, R.; Shinton, S.A.; Martin, E.S.; Koval, A.; Calin, G.A.; Cesari, R.; Russo, G.; Hardy, R.R.; Croce, C.M. Human Chronic Lymphocytic Leukemia Modeled in Mouse by Targeted TCL1 Expression. *Proc. Natl. Acad. Sci.* **2002**, *99*, 6955–6960, doi:10.1073/pnas.102181599.
20. Bertilaccio, M.T.S.; Scielzo, C.; Simonetti, G.; Ponzoni, M.; Apollonio, B.; Fazi, C.; Scarfò, L.; Rocchi, M.; Muzio, M.; Caligaris-Cappio, F.; et al. A Novel Rag2−/−γc−/−-Xenograft Model of Human CLL. *Blood* **2010**, *115*, 1605–1609, doi:10.1182/blood-2009-05-223586.
21. Patten, P.E.M.; Ferrer, G.; Chen, S.-S.; Kolitz, J.E.; Rai, K.R.; Allen, S.L.; Barrientos, J.C.; Ioannou, N.; Ramsay, A.G.; Chiorazzi, N. A Detailed Analysis of Parameters Supporting the Engraftment and Growth of Chronic Lymphocytic Leukemia Cells in Immune-Deficient Mice. *Front. Immunol.* **2021**, *12*.

22. Klein, U.; Lia, M.; Crespo, M.; Siegel, R.; Shen, Q.; Mo, T.; Ambesi-Impiombato, A.; Califano, A.; Migliazza, A.; Bhagat, G.; et al. The DLEU2/MiR-15a/16-1 Cluster Controls B Cell Proliferation and Its Deletion Leads to Chronic Lymphocytic Leukemia. *Cancer Cell* **2010**, *17*, 28–40, doi:10.1016/j.ccr.2009.11.019.
23. ten Hacken, E.; Wu, C.J. Understanding CLL Biology through Mouse Models of Human Genetics. *Blood* **2021**, *138*, 2621–2631, doi:10.1182/blood.2021011993.
24. Hobbs, G.A.; Der, C.J.; Rossman, K.L. RAS Isoforms and Mutations in Cancer at a Glance. *J. Cell Sci.* **2016**, *129*, 1287–1292, doi:10.1242/jcs.182873.
25. Malumbres, M.; Barbacid, M. RAS Oncogenes: The First 30 Years. *Nat. Rev. Cancer* **2003**, *3*, 459–465, doi:10.1038/nrc1097.
26. Liu, W.N.; Yan, M.; Chan, A.M. A Thirty-Year Quest for a Role of R-Ras in Cancer: From an Oncogene to a Multitasking GTPase. *Cancer Lett.* **2017**, *403*, 59–65, doi:10.1016/j.canlet.2017.06.003.
27. Graham, S.M.; Oldham, S.M.; Martin, C.B.; Drugan, J.K.; Zohn, I.E.; Campbell, S.; Der, C.J. TC21 and Ras Share Indistinguishable Transforming and Differentiating Activities. *Oncogene* **1999**, *18*, 2107–2116, doi:10.1038/sj.onc.1202517.
28. Graham, S.M.; Cox, A.D.; Drivas, G.; Rush, M.G.; D'Eustachio, P.; Der, C.J. Aberrant Function of the Ras-Related Protein TC21/R-Ras2 Triggers Malignant Transformation. *Mol. Cell. Biol.* **1994**, *14*, 4108–4115, doi:10.1128/mcb.14.6.4108-4115.1994.
29. Movilla, N.; Crespo, P.; Bustelo, X.R. Signal Transduction Elements of TC21, an Oncogenic Member of the R-Ras Subfamily of GTP-Binding Proteins. *Oncogene* **1999**, *18*, 5860–5869, doi:10.1038/sj.onc.1202968.
30. Janapati, S.; Wurtzel, J.; Dangelmaier, C.; Manne, B.K.; Bhavanasi, D.; Kostyak, J.C.; Kim, S.; Holinstat, M.; Kunapuli, S.P.; Goldfinger, L.E. TC21/RRas2 Regulates Glycoprotein VI–FcRγ-Mediated Platelet Activation and Thrombus Stability. *J. Thromb. Haemost.* **2018**, *16*, 1632–1645, doi:10.1111/jth.14197.
31. Huang, Y.; Rangwala, F.; Fulkerson, P.C.; Ling, B.; Reed, E.; Cox, A.D.; Kamholz, J.; Ratner, N. Role of TC21/R-Ras2 in Enhanced Migration of Neurofibromin-Deficient Schwann Cells. *Oncogene* **2004**, *23*, 368–378, doi:10.1038/sj.onc.1207075.
32. Larive, R.M.; Abad, A.; Cardaba, C.M.; Hernández, T.; Cañamero, M.; de Álava, E.; Santos, E.; Alarcón, B.; Bustelo, X.R. The Ras-like Protein R-Ras2/TC21 Is Important for Proper Mammary Gland Development. *Mol. Biol. Cell* **2012**, *23*, 2373–2387, doi:10.1091/mbc.e12-01-0060.
33. Macha, M.A.; Matta, A.; Sriram, U.; Thakkar, A.; Shukla, N.K.; Datta Gupta, S.; Ralhan, R. Clinical Significance of TC21 Overexpression in Oral Cancer. *J. Oral Pathol. Med.* **2010**, *39*, 477–485, doi:10.1111/j.1600-0714.2009.00854.x.
34. Sharma, R.; Sud, N.; Chattopadhyay, T.K.; Ralhan, R. TC21/R-Ras2 Upregulation in Esophageal Tumorigenesis: Potential Diagnostic Implications. *Oncology* **2005**, *69*, 10–18, doi:10.1159/000087283.
35. Luo, H.; Hao, X.; Ge, C.; Zhao, F.; Zhu, M.; Chen, T.; Yao, M.; He, X.; Li, J. TC21 Promotes Cell Motility and Metastasis by Regulating the Expression of E-Cadherin and N-Cadherin in Hepatocellular Carcinoma. *Int. J. Oncol.* **2010**, *37*, 853–859, doi:10.3892/ijo_00000736.
36. Lee, J.H.; Pyon, J.-K.; Lee, S.H.; Lee, Y.J.; Kang, S.G.; Kim, C.H.; Kim, D.W.; Nam, H.S.; Park, Y.H.; Jeong, D.J.; et al. Greater Expression of TC21/R-Ras2 in Highly Aggressive Malignant Skin Cancer. *Int. J. Dermatol.* **2011**, *50*, 956–960, doi:10.1111/j.1365-4632.2010.04846.x.
37. Larive, R.M.; Moriggi, G.; Menacho-Márquez, M.; Cañamero, M.; Álava, E. de; Alarcón, B.; Dosil, M.; Bustelo, X.R. Contribution of the R-Ras2 GTP-Binding Protein to Primary Breast Tumorigenesis and Late-Stage Metastatic Disease. *Nat. Commun.* **2014**, *5*, 3881, doi:10.1038/ncomms4881.
38. Clark, G.J.; Kinch, M.S.; Gilmer, T.M.; Burridge, K.; Der, C.J. Overexpression of the Ras-Related TC21/R-Ras2 Protein May Contribute to the Development of Human Breast Cancers. *Oncogene* **1996**, *12*, 169–176.
39. Capri, Y.; Flex, E.; Krumbach, O.H.F.; Carpentieri, G.; Cecchetti, S.; Lißewski, C.; Rezaei Adariani, S.; Schanze, D.; Brinkmann, J.; Piard, J.; et al. Activating Mutations of RRAS2 Are a Rare Cause of Noonan Syndrome. *Am. J. Hum. Genet.* **2019**, *104*, 1223–1232, doi:10.1016/j.ajhg.2019.04.013.
40. Niihori, T.; Nagai, K.; Fujita, A.; Ohashi, H.; Okamoto, N.; Okada, S.; Harada, A.; Kihara, H.; Arbogast, T.; Funayama, R.; et al. Germline-Activating RRAS2 Mutations Cause Noonan Syndrome. *Am. J. Hum. Genet.* **2019**, *104*, 1233–1240, doi:10.1016/j.ajhg.2019.04.014.
41. Fernández-Pisonero, I.; Clavaín, L.; Robles-Valero, J.; Lorenzo-Martín, L.F.; Caloto, R.; Nieto, B.; García-Macías, C.; Oeste, C.L.; Sánchez-Martín, M.; Abad, A.; et al. A Hotspot Mutation Targeting the R-RAS2 GTPase Acts as a Potent Oncogenic Driver in a Wide Spectrum of Tumors. *Cell Rep.* **2022**, *38*, 110522, doi:10.1016/j.celrep.2022.110522.
42. Clavaín, L.; Fernández-Pisonero, I.; Movilla, N.; Lorenzo-Martín, L.F.; Nieto, B.; Abad, A.; García-Navas, R.; Llorente-González, C.; Sánchez-Martín, M.; Vicente-Manzanares, M.; et al. Characterization of Mutant Versions of the R-RAS2/TC21 GTPase Found in Tumors. *Oncogene* **2022**, 1–17, doi:10.1038/s41388-022-02563-9.
43. Delgado, P.; Cubelos, B.; Calleja, E.; Martínez-Martín, N.; Ciprés, A.; Mérida, I.; Bellas, C.; Bustelo, X.R.; Alarcón, B. Essential Function for the GTPase TC21 in Homeostatic Antigen Receptor Signaling. *Nat. Immunol.* **2009**, *10*, 880–888, doi:10.1038/ni.1749.

44. Martínez-Martín, N.; Fernández-Arenas, E.; Cemerski, S.; Delgado, P.; Turner, M.; Heuser, J.; Irvine, D.J.; Huang, B.; Bustelo, X.R.; Shaw, A.; et al. T Cell Receptor Internalization from the Immunological Synapse Is Mediated by TC21 and RhoG GTPase-Dependent Phagocytosis. *Immunity* **2011**, *35*, 208–222, doi:10.1016/j.immuni.2011.06.003.
45. Mendoza, P.; Martínez-Martín, N.; Bovolenta, E.R.; Reyes-Garau, D.; Hernansanz-Agustín, P.; Delgado, P.; Diaz-Muñoz, M.D.; Oeste, C.L.; Fernández-Pisonero, I.; Castellano, E.; et al. R-Ras2 Is Required for Germinal Center Formation to Aid B Cells during Energetically Demanding Processes. *Sci. Signal.* **2018**, *11*, eaal1506, doi:10.1126/scisignal.aal1506.
46. Hortal, A.M.; Oeste, C.L.; Cifuentes, C.; Alcoceba, M.; Fernández-Pisonero, I.; Clavaín, L.; Tercero, R.; Mendoza, P.; Domínguez, V.; García-Flores, M.; et al. Overexpression of Wild Type RRAS2, without Oncogenic Mutations, Drives Chronic Lymphocytic Leukemia. *Mol. Cancer* **2022**, *21*, 35, doi:10.1186/s12943-022-01496-x.
47. Thai, T.-H.; Calado, D.P.; Casola, S.; Ansel, K.M.; Xiao, C.; Xue, Y.; Murphy, A.; Frendewey, D.; Valenzuela, D.; Kutok, J.L.; et al. Regulation of the Germinal Center Response by MicroRNA-155. *Science* **2007**, *316*, 604–608, doi:10.1126/science.1141229.
48. Hobeika, E.; Thiemann, S.; Storch, B.; Jumaa, H.; Nielsen, P.J.; Pelanda, R.; Reth, M. Testing Gene Function Early in the B Cell Lineage in Mb1-Cre Mice. *Proc. Natl. Acad. Sci.* **2006**, *103*, 13789–13794, doi:10.1073/pnas.0605944103.
49. Hacken, E. ten; Sivina, M.; Kim, E.; O'Brien, S.; Wierda, W.G.; Ferrajoli, A.; Estrov, Z.; Keating, M.J.; Oellerich, T.; Scielzo, C.; et al. Functional Differences Between IgM and IgD Signaling in Chronic Lymphocytic Leukemia. *J. Immunol. Baltim. Md 1950* **2016**, *197*, 2522–2531, doi:10.4049/jimmunol.1600915.
50. Damle, R.N.; Ghiotto, F.; Valetto, A.; Albesiano, E.; Fais, F.; Yan, X.-J.; Sison, C.P.; Allen, S.L.; Kolitz, J.; Schulman, P.; et al. B-Cell Chronic Lymphocytic Leukemia Cells Express a Surface Membrane Phenotype of Activated, Antigen-Experienced B Lymphocytes: Presented in Part at the 42nd Annual Meeting of the American Society of Hematology, December 1-5, 2000, San Francisco, CA. *Blood* **2002**, *99*, 4087–4093, doi:10.1182/blood.V99.11.4087.
51. Kutsch, N.; Fink, A.M.; Fischer, K. Management of Front Line Chronic Lymphocytic Leukemia. *Am. J. Hematol.* **2022**, *97*, S3–S10, doi:10.1002/ajh.26677.
52. Hallek, M.; Al-Sawaf, O. Chronic Lymphocytic Leukemia: 2022 Update on Diagnostic and Therapeutic Procedures. *Am. J. Hematol.* **2021**, *96*, 1679–1705, doi:10.1002/ajh.26367.
53. Barr, P.M.; Robak, T.; Owen, C.; Tedeschi, A.; Bairey, O.; Bartlett, N.L.; Burger, J.A.; Hillmen, P.; Coutre, S.; Devereux, S.; et al. Sustained Efficacy and Detailed Clinical Follow-up of First-Line Ibrutinib Treatment in Older Patients with Chronic Lymphocytic Leukemia: Extended Phase 3 Results from RESONATE-2. *Haematologica* **2018**, *103*, 1502–1510, doi:10.3324/haematol.2018.192328.
54. Mayerhoefer, M.E.; Haug, A.; Jäger, U.; Pichler, V.; Pfaff, S.; Wester, H.-J.; Hacker, M.; Kazianka, L.; Staber, P.B. In Human Visualization of Ibrutinib-Induced CLL Compartment Shift. *Cancer Immunol. Res.* **2020**, *8*, 984–989, doi:10.1158/2326-6066.CIR-19-0880.
55. Coutre, S.; Choi, M.; Furman, R.R.; Eradat, H.; Heffner, L.; Jones, J.A.; Chyla, B.; Zhou, L.; Agarwal, S.; Waskiewicz, T.; et al. Venetoclax for Patients with Chronic Lymphocytic Leukemia Who Progressed during or after Idelalisib Therapy. *Blood* **2018**, *131*, 1704–1711, doi:10.1182/blood-2017-06-788133.
56. Kater, A.P.; Slinger, E.; Cretenet, G.; Martens, A.W.; Balasubramanian, S.; Leverson, J.D.; Eldering, E. Combined Ibrutinib and Venetoclax Treatment vs Single Agents in the TCL1 Mouse Model of Chronic Lymphocytic Leukemia. *Blood Adv.* **2021**, *5*, 5410–5414, doi:10.1182/bloodadvances.2021004861.
57. Burger, J.A.; Landau, D.A.; Taylor-Weiner, A.; Bozic, I.; Zhang, H.; Sarosiek, K.; Wang, L.; Stewart, C.; Fan, J.; Hoellenriegel, J.; et al. Clonal Evolution in Patients with Chronic Lymphocytic Leukaemia Developing Resistance to BTK Inhibition. *Nat. Commun.* **2016**, *7*, 11589, doi:10.1038/ncomms11589.
58. Woyach, J.A.; Furman, R.R.; Liu, T.-M.; Ozer, H.G.; Zapatka, M.; Ruppert, A.S.; Xue, L.; Li, D.H.-H.; Steggerda, S.M.; Versele, M.; et al. Resistance Mechanisms for the Bruton's Tyrosine Kinase Inhibitor Ibrutinib. *N. Engl. J. Med.* **2014**, *370*, 2286–2294, doi:10.1056/NEJMoa1400029.